small tumors and metastases and possibly in schemes designed to specifically target chemotoxic therapy to tumor vasculature.

References and Notes

1. J. Folkman, *N. Engl. J. Med.* **285**, 1182 (1971).
2. ———, *J. Natl. Cancer Inst.* **82**, 4 (1990).
3. D. Hanahan and J. Folkman, *Cell* **86**, 353 (1996).
4. P. Wesseling, J. A. van der Laak, H. de Leeuw, D. J. Ruiter, P. C. Burger, *J. Neurosurg.* **81**, 902 (1994); L. Holmgren, M. S. O'Reilly, J. Folkman, *Nature Med.* **1**, 149 (1995); F. Pezzella, *et al.*, *Am. J. Pathol.* **151**, 1417 (1997).
5. D. J. Dumont, T. P. Yamaguchi, R. A. Conlon, J. Rossant, M. L. Breitman, *Oncogene* **7**, 1471 (1992); J. Partanen *et al.*, *Mol. Cell. Biol.* **12**, 1698 (1992); A. Iwama *et al.*, *Biochem. Biophys. Res. Commun.* **195**, 301 (1993); P. C. Maisonpierre, M. Goldfarb, G. D. Yancopoulos, G. Gao, *Oncogene* **8**, 1631 (1993); T. N. Sato, Y. Qin, C. A. Kozak, K. L. Audus, *Proc. Natl. Acad. Sci. U.S.A.* **90**, 9355 (1993); H. Schnurch and W. Risau, *Development* **119**, 957 (1993); S. F. Ziegler, T. A. Bird, S. A. Schneringer, K. A. Schooley, P. R. Baum, *Oncogene* **8**, 663 (1993); N. Ferrara, *Curr. Top. Microbiol. Immunol.* **237**, 1 (1999).
6. D. J. Dumont *et al.*, *Genes Dev.* **8**, 1897 (1994); T. N. Sato *et al.*, *Nature* **376**, 70 (1995).
7. S. Davis *et al.*, *Cell* **87**, 1161 (1996).
8. C. Suri *et al.*, *ibid.*, p. 1171.
9. P. C. Maisonpierre *et al.*, *Science* **277**, 55 (1997).
10. D. Valenzuela *et al.*, *Proc. Natl. Acad. Sci. U.S.A.* **96**, 1904 (1999).
11. A diagram depicting the complementary and coordinated roles of VEGF and the angiopoietins during vascular growth and development can be found at *Science* Online (Web Fig. 1 at www.sciencemag.org/feature/data/1039904.shl).
12. F. Shalaby *et al.*, *Nature* **376**, 62 (1995); P. Carmeliet *et al.*, *ibid.* **380**, 435 (1996); N. Ferrara *et al.*, *ibid.*, p. 439.
13. C. Suri *et al.*, *Science* **282**, 468 (1998).
14. A. Wong *et al.*, *Circ. Res.* **81**, 567 (1997).
15. D. Shweiki, M. Neeman, A. Itin, E. Keshet, *Proc. Natl. Acad. Sci. U.S.A.* **92**, 768 (1995).
16. K. J. Kim *et al.*, *Nature* **362**, 841 (1993); B. Millauer, L. K. Shawver, K. H. Plate, W. Risau, A. Ullrich, *ibid.* **367**, 576 (1994); R. S. Warren, H. Yuan, M. R. Matli, N. A. Gillett, N. Ferrara, *J. Clin. Invest.* **95**, 1789 (1995); B. Millauer *et al.*, *Cancer Res.* **56**, 1615 (1996); C. K. Goldman *et al.*, *Proc. Natl. Acad. Sci. U.S.A.* **95**, 8795 (1998).
17. N. Nagano, H. Sasaki, M. Aoyagi, K. Hirakawa, *Acta Neuropathol.* **86**, 117 (1993).
18. B. Enholm *et al.*, *Oncogene* **14**, 2475 (1997).
19. A figure showing the expression patterns of Tie1, Tie2, Ang-1, Ang-2, and VEGF in early rat C6 gliomas can be found at *Science* Online (Web Fig. 2 at www.sciencemag.org/feature/data/1039904.shl).
20. A. Stratmann, W. Risau, K. H. Plate, *Am. J. Pathol.* **153**, 1459 (1998).
21. A complete description of angiopoietin expression in human glioblastomas can be found at *Science* Online (Web Fig. 3 at www.sciencemag.org/feature/data/1039904.shl); D. Zagzag *et al.*, *Exp. Neurol.*, in press.
22. J. Holash *et al.*, unpublished observations; D. Zagzag *et al.*, unpublished observations.
23. L. Benjamin, D. Golijanin, A. Itin, D. Pode, E. Keshet, *J. Clin. Invest.* **103**, 159 (1999).
24. S. Tanaka *et al.*, *ibid.*, p. 341.
25. S. D. Morgenbesser *et al.*, *EMBO J.* **14**, 743 (1995).
26. J. K. Morse *et al.*, *J. Neurosci.* **13**, 4146 (1993).
27. D. M. Valenzuela *et al.*, *Neuron* **10**, 963 (1993).
28. Tumor cells were obtained from the American Type Culture Collection and grown in culture. About 1.0×10^5 C6 or RBA cells were suspended in ~2 μl of phosphate-buffered saline (PBS) and injected stereotaxically over a period of 5 to 10 min into the right striatum (AP + 0.5; ML −3.0; DV −6.0 relative to Bregma) of adult male Sprague-Dawley rats. About 5.0×10^5 Lewis lung carcinoma cells were suspended in 50 μl of serum-free media and injected into the jugular vein of adult male C57Bl mice.
29. Animals were anesthetized and either decapitated or perfused with 4% paraformaldehyde. Brains for thick sliding microtome sections (40 μm) were post-fixed in 4% paraformaldehyde overnight and then equilibrated in 35% sucrose. Fixed brains for thin sections (10 μm) were equilibrated in 17% sucrose. Fixed and fresh brains were frozen in methylbutane, chilled in dry ice, and sectioned on a cryostat. For TUNEL labeling (*25*), brains were immersion-fixed in 10% neutral buffered formalin and embedded in paraffin. Fixed sections were immunostained with a monoclonal antibody to rat endothelial cell antigen (RECA1; 1:250; Serotec) and a biotinylated horse anti-mouse secondary antibody (1:1500; Vector) or with a monoclonal antibody to PECAM (CD31; 1:100; Pharmingen) and a biotinylated rabbit anti-rat secondary antibody (1:150; Vector) as previously described (*26*). A similar protocol was used for double labeling. Sections were initially labeled with a monoclonal antibody to alpha smooth muscle actin (SMA; 1:500; DAKO) and a biotinylated goat anti-mouse immunoglobulin G IIa secondary antibody (1:1250; Amersham). SMA staining was visualized with a Vectastain Elite kit (Vector), and a black reaction product was generated by nickel sulfate enhancement. After SMA labeling, sections were then reblocked and labeled with antibody to RECA (1:100). A brown reaction product was used.
30. Human umbilical vein endothelial cells (HUVECs) (Clonetics, San Diego, CA) were maintained in recommended medium on gelatin-coated plastic. For DNA synthesis assays, 1×10^4 cells were plated in 96-well microwells and grown for 24 hours in basal medium plus 0.5% fetal bovine serum. Cells were re-fed with the same medium plus purified factors and grown for 20 hours, with 1 mCi tritiated thymidine (80 Ci/mmol; Amersham) being present for the last 3 hours of incubation. Cells were rinsed and fixed with trichloroacetic acid, and thymidine incorporation was measured by standard liquid scintillation techniques. Ang-1* (ANG1*) was a modified form of human Ang-1, described previously (*9*); VEGF was murine VEGF-164, produced and purified from baculovirus-infected insect cells; bFGF was human basic fibroblast growth factor (R&D Systems). For assessing resistance to apoptosis, plates of ~80% confluent HUVECs were rinsed twice with basal medium and grown for 18 to 20 hours in basal medium and bovine serum albumin (0.5 mg/ml), plus or minus purified factors. Both adherent and nonadherent cells were harvested, pooled, and fixed in 70% ethanol at −20°C overnight. Cells were washed in PBS, incubated for 30 min with ribonuclease A (5 kunitz units/ml; Sigma) and propidium iodide (50 μg/ml; Sigma). Cellular DNA content, as judged by propidium iodide fluorescence, was measured by flow cytometry (MoFlo, Cytomation, Fort Collins, CO).
31. A. Papapetropoulos *et al.*, *Lab. Invest.* **79**, 213 (1999).
32. Fresh frozen or fixed sections were probed with ^{35}S-labeled cRNAs (*27*). Probes for VEGF and Ang-1 and Ang-2 have been described (*9*). For Tie1, a 1.3-kb fragment of rat Tie1 spanning the last 309 codons and 375 base pairs of the 3′ untranslated sequence was used, and for Tie2 a 460–base pair fragment spanning codons 771 through 924 within the kinase domain was used. This probe does not cross-hybridize to Tie1 mRNA in Northern blots.

33. We thank B. Luan, J. Zheng, P. Burfeind, S. Zabski, and F. Martin for excellent technical assistance; E. Burrows and C. Murphy for graphics work; A. Hooper and D. Friedlander for data on human gliomas; and M. Grumet for intellectual discussions. Supported in part by a grant from the Children's Brain Tumor Foundation to D.Z. and by Procter & Gamble Pharmaceuticals, Inc. All animal studies were done in accordance with institutional guidelines.

9 March 1999; accepted 10 May 1999

Initiation of Mammalian Liver Development from Endoderm by Fibroblast Growth Factors

Joonil Jung,[1] Minghua Zheng,[1] Mitchell Goldfarb,[2] Kenneth S. Zaret[1]*

The signaling molecules that elicit embryonic induction of the liver from the mammalian gut endoderm or induction of other gut-derived organs are unknown. Close proximity of cardiac mesoderm, which expresses fibroblast growth factors (FGFs) 1, 2, and 8, causes the foregut endoderm to develop into the liver. Treatment of isolated foregut endoderm from mouse embryos with FGF1 or FGF2, but not FGF8, was sufficient to replace cardiac mesoderm as an inducer of the liver gene expression program, the latter being the first step of hepatogenesis. The hepatogenic response was restricted to endoderm tissue, which selectively coexpresses FGF receptors 1 and 4. Further studies with FGFs and their specific inhibitors showed that FGF8 contributes to the morphogenetic outgrowth of the hepatic endoderm. Thus, different FGF signals appear to initiate distinct phases of liver development during mammalian organogenesis.

Identifying the molecular signals that initiate organogenesis from the gut is important for understanding the fundamental mechanisms of developmental regulation, hereditary digestive disorders, and tissue regeneration. Different segments of the mammalian gut endoderm give rise to the liver, lung, pancreas, thyroid, and gastrointestinal tract. Typically, a portion of the endoderm will begin to express genes specific to one of these tissues, and then the newly specified cells will proliferate out of the endoderm layer to form a tissue bud, initiating morphogenesis (*1, 2*). In *Drosophila*, the initial specification of tissues

[1]Department of Molecular Biology, Cell Biology, and Biochemistry, Brown University, Box G-J363, Providence, RI 02912, USA. [2]Brookdale Center for Molecular Biology, Mount Sinai School of Medicine, New York, NY 10029, USA.

*To whom correspondence should be addressed: E-mail: zaret@brown.edu

within the gut endoderm is caused by signals from overlying mesoderm (*3*). In the chick, transplanted foregut endoderm will develop into liver only if it is with its adjacent cardiac mesoderm (*4*); mesoderm from other areas of the embryo is not hepatogenic (*4, 5*). Gene inactivation studies in mice have identified many signaling molecules and transcription factors that are required for development of gut-derived organs, but the factors are critical either for the formation of the endoderm itself (*6*) or for tissue development after the morphogenetic bud stage (*7*), leaving open the question of how the tissue types are initially specified.

We have modified the tissue transplantation approach to identify signals that control the initial specification of the liver. The first known evidence of hepatic differentiation of the ventral foregut endoderm is activation of the liver-specific serum albumin gene and enhanced expression of α-fetoprotein (AFP) mRNA at the seven- to eight-somite stage in the mouse (*2*). Transcription of these genes in embryo tissues is detectable by reverse-transcriptase polymerase chain reaction (RT-PCR) analysis of RNA (*2*); specific mRNA accumulation at this stage has not been detectable by in situ hybridization (*2, 8*). Later in development, the newly specified hepatic cells exhibit morphogenetic outgrowth to form the liver bud (*2, 8*). When ventral foregut endoderm is isolated from

Table 1. Induction of hepatic mRNAs in embryo tissue cultures. Cumulative number of embryo tissue fragments in our laboratory that expressed (+) or did not express (−) mRNAs for the designated liver-specific genes after 48 hours in culture, as assayed by RT-PCR, is indicated. ND, not done.

Culture conditions	Albumin		AFP		TTR	
	−	+	−	+	−	+
Ventral endoderm (VE)	20*	0	4	0	3	0
VE + heparan sulfate	19	0	7	1	4	1
VE + cardiac mesoderm (CM)	0	34†	0	17‡	1	8
VE + FGF1 (50 to 500 ng ml^{-1})	1	11	0	8†	0	3†
VE + FGF1 (5 ng ml^{-1})	4	5	4	2	ND	ND
VE + FGF2 (50 ng ml^{-1})	6	1	ND	ND	ND	ND
VE + FGF2 (5 ng ml^{-1})	2	8	0	2	0	3
VE + FGF8b (50 ng ml^{-1})	7	3	ND	ND	ND	ND
VE + FGF8b (5 ng ml^{-1})	4	2	0	1	1	2
Ectodermal and mesodermal tissues§						
FGF1 (50 to 500 ng ml^{-1})	7	0	1	0	ND	ND
FGF2 (5 ng ml^{-1})	9¶	0	ND	ND	ND	ND

*Includes 17 samples from (*2*). †Includes 21 samples from (*2*). ‡Includes 13 samples from (*2*). §Includes neural tube, midsections, and head tissues. ¶Three samples exhibited trace amounts of albumin RT-PCR product, consistent with the very small amount of albumin mRNA in certain heterologous tissues (*32*).

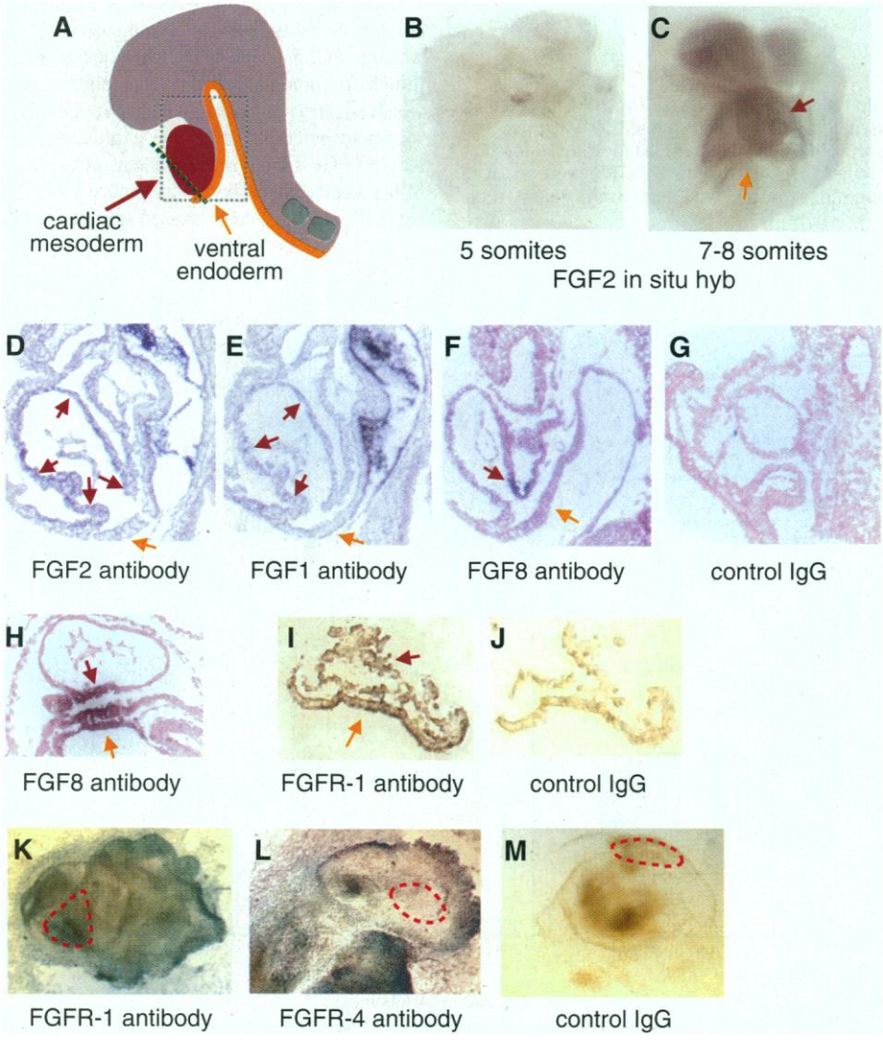

Fig. 1. Expression patterns of FGF signaling molecules in five- to eight-somite mouse embryos. (**A**) Side view of mouse embryo at the seven- to eight-somite stage. Squared region indicates sections viewed in (D) to (G); dashed line indicates orthogonal section in (H) to (J). (**B** and **C**) FGF2 in situ hybridization (*19*); front view of embryos with optic lobes at top. MRNA-positive cardiac region is denoted by red arrow. Note the lack of staining in the endodermal lip beneath the cardiac region (orange arrow). (**D** to **J**) Antibody staining of seven- to eight-somite embryo sections. Red arrows denote FGF-positive segments of the cardiac region. Orange arrows denote ventral foregut endoderm. Nonspecific, dark staining was occasionally observed in the foregut pocket (D and E). Normal mouse IgG was used as a control in (G); normal rabbit IgG was used in (J). (H) Localized FGF8 staining at the boundary between the cardiac mesoderm and the ventral foregut endoderm from an embryo sectioned orthogonal to the arrows in (F). (**K** to **M**) Antibody staining of cocultures of ventral foregut endoderm and cardiac mesoderm. Dashed circles represent areas of beating cardiac tissue. FGFR-1 was present throughout the culture, whereas FGFR-4 was present outside the cardiac areas and was especially prominent at the leading edge of the explants.

mouse embryos at ~8.25 days of gestation (two- to six-somite stages; Fig. 1A) and cultured in microwells for 2 days, expression of albumin mRNA is activated and the amount of AFP mRNA is increased only if the endoderm is in contact with cardiac mesoderm (*2*). Cardiac mesoderm in the same microwell as the endodermal cells, but separated from the latter, fails to induce liver gene expression, which indicates that either cell contact or one or more locally secreted factors is critical (*2*). Hepatic induction in this in vitro assay system is similar to that in chicken endoderm transplantation studies (*4, 5*). In both chicken and mouse embryos, endogenous hepatic induction by the cardiac mesoderm takes place at about the seven-somite stage (*2, 4*).

We investigated the role of fibroblast growth factors (FGFs) as potential hepatogenic signals because chicken embryos express FGF1 and FGF2 in the myocardium at the 7- to 13-somite stages (*9*) and mouse embryos express FGF8 mRNA in the cardiac mesoderm from the presomitic to the 7-somite stage (*10*). Also, FGF receptor 4 (FGFR-4) mRNA is expressed exclusively in the endoderm at 8.5 days of gestation in mice (*11*) and FGFR-1 is in both the cardiac and endoderm regions (*12*). FGFs are secreted locally into the extracellular matrix (*13*) and can promote differentiation of the embryonic mesoderm (*14*) and the anterior pituitary (*15*) as well as induce morphogenesis of limbs, lungs, and teeth (*16*). Inactivation of the FGFR-1 and FGF8 genes results in early embryonic lethality before hepatogenesis (*17*), whereas FGFR-4 and FGF2 gene inactivation results in minimal embryonic phenotypes, which suggests redundancy (*18*). We therefore sought to precisely define the expression patterns of FGF signaling components at the time of hepatogenesis in the mouse embryo.

FGF2 mRNA was expressed strongly in the

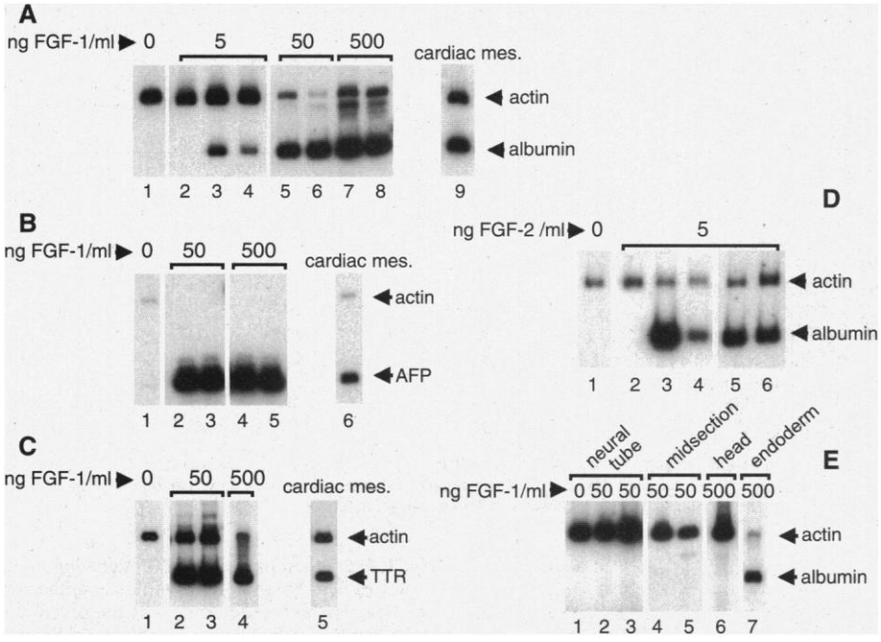

Fig. 2. Induction of liver gene expression in ventral endoderm cultures treated with FGFs. (**A** to **D**) RT-PCR analysis of RNA from ventral endoderm tissues cultured for 2 days either with heparan sulfate (50 ng ml^{-1}) and the designated concentrations of FGFs or with cardiac mesoderm (cardiac mes.). Actin and liver-specific mRNA for albumin (A and D), AFP (B), or TTR (C) were assayed simultaneously. (**E**) Failure of FGF1 to induce albumin expression in embryonic neural tube, midsections, and head tissues.

Fig. 3. Soluble dominant-negative FGF receptor fusion proteins can inhibit albumin gene induction in foregut cocultures. (**A**) FR-IgG fusion protein strategy. Loops denote immunoglobulin-like domains; thick bars denote tyrosine kinase domain; zigzag denotes hinge domain; and V and C denote variable and constant domains of IgG heavy chain. (**B**) SDS-PAGE with silver stain of FR1-IgG and FR4-IgG purified from COS-7 cell supernatants compared with IgG. Mock denotes material from mock-transfected cells. (**C**) Immunoblot analysis of NIH 3T3 cell lysate after cell incubation for 5 hours with FGFs and FR-IgGs as shown. Lane 2, untreated cell lysate showed basal level of protein phosphorylation. Lanes 3 and 6, treatment with FGF2 or FGF8b caused a shift in the phosphoprotein profile. (**D** to **F**) Summary of RT-PCR analysis of albumin gene expression, relative to actin, in cocultures of ventral endoderm and cardiac mesoderm in the presence of FR-IgG at either 500 or 200 ng ml^{-1} with heparan sulfate at 100 ng ml^{-1}. Similar results were obtained from either condition; results were pooled. For a control, we used the same amount of human IgG or plain buffer.

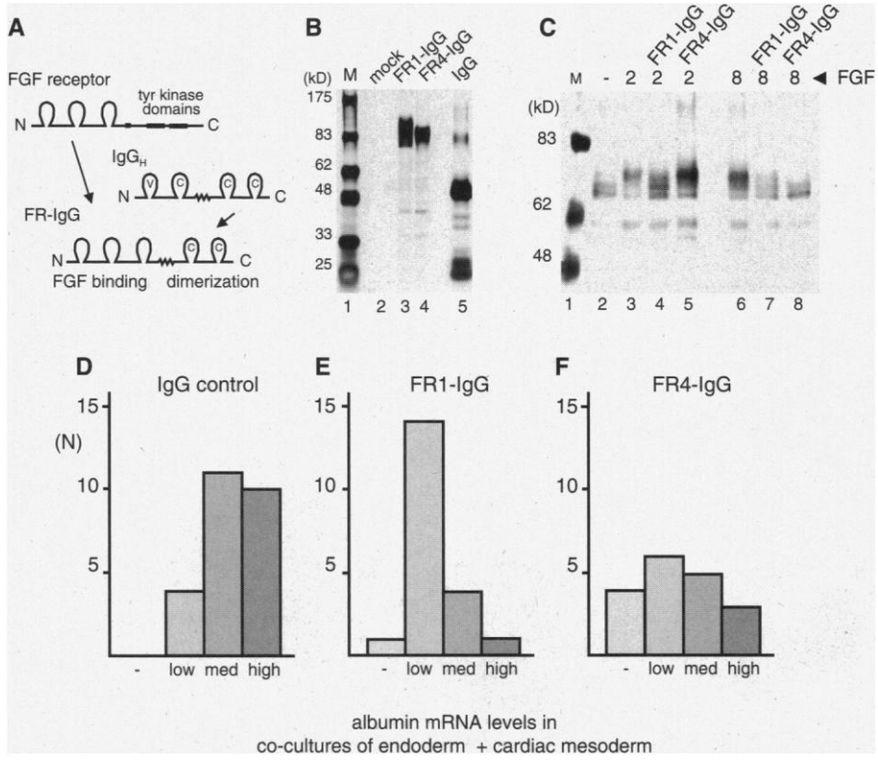

cardiac region at the seven- to eight-somite stage (Fig. 1C, red arrow) but not in the endoderm below the cardiac region (Fig. 1C, orange arrow) (*19*). FGF2 mRNA was barely detectable at the five-somite stage (Fig. 1B), which shows that it is induced at the time of hepatogenesis. To address whether FGFs themselves are present in the cardiac mesoderm, we used antibodies to stain mouse embryo sections at the seven- to eight-somite stage (*20*). FGF2 was expressed throughout the cardiac mesoderm (Fig. 1D, red arrows) adjacent to the ventral foregut endoderm (Fig. 1D, orange arrow; Fig. 1G, control). Although Crossley and Martin (*10*) and we (*21*) found that cardiac mesoderm expression of FGF8 mRNA declines by the seven-somite stage, we found that FGF8 antigen persists in the cardiac mesoderm near the endoderm (Fig. 1F, red arrow). Interestingly, there was very localized and intense FGF8 staining at the boundary between the cardiac mesoderm and the endoderm (Fig. 1H, red and orange arrows, respectively). FGF1 staining of the cardiac mesoderm was just beginning to appear in seven- to eight-somite embryos (Fig. 1E) and was undetectable at earlier stages (*21*). FGFR-1 was present in the foregut endoderm as well as in the cardiac mesoderm (Fig. 1I, red and orange arrows; Fig. 1J, control). We also found that FGFR-1 and FGFR-4 are expressed abundantly in the endodermal/epithelial portions of cocultures of ventral foregut endoderm and cardiac mesoderm (Fig. 1, K and L; Fig. 1M, control). We conclude that multiple FGF signaling components are expressed in the relevant tissues precisely at the time of hepatogenesis.

To test whether FGFs alone are sufficient to induce the first step of hepatogenesis, we isolated ventral foregut endoderm from two- to six-somite stage mouse embryos (*22*) and treated the cells with or without FGFs in the presence of a heparan sulfate carrier (*23*). Tissue explants were cultured in microwells for 2 days, and then RNA was isolated from individual explants and analyzed for liver gene expression by RT-PCR (*24*). Of 39 control endoderm explants cultured alone, without FGFs, including 19 tissues grown in the presence of the heparan sulfate carrier, none expressed serum albumin mRNA (Fig. 2A, lane 1; Table 1). Only 1 of 12 tissues was AFP-positive (Table 1). In contrast, of a total of 12 ventral foregut endoderm tissues grown in the presence of FGF-1 (50 or 500 ng ml^{-1}), 11 expressed albumin mRNA and of the 8 tested all expressed AFP mRNA (Fig. 2A, lanes 5 to 8; Fig. 2B, lanes 2 to 5; Table 1). Of nine ventral endoderm fragments cultured in the presence of FGF1 at 5 ng ml^{-1}, five exhibited albumin mRNA expression (Fig. 2A, lanes 2 to 4; Table 1). This FGF1 concentration is known to be close to the threshold for cell responses (*25*). Although FGF2 at 50 ng ml^{-1} was inefficient (Table 1), FGF2 at 5 ng ml^{-1} efficiently induced albumin (Fig. 2D, lanes 2 to 6; Table 1). Such sharp dosage thresholds with FGF2 have been well documented (*26*). FGF8b was inefficient in albumin induction at either 5 or 50 ng ml^{-1} (Table 1). As a third marker for hepatogenesis, we analyzed the expression of transthyretin (TTR) mRNA, which is expressed in both the yolk sac and early liver (*27*). TTR mRNA was detectable by RT-PCR throughout the endoderm during the two- to eight-somite stages (*21*) and its expression was extinguished when the endoderm was cultured alone (Fig. 2C, lane 1). However, treating the endoderm with FGF1 maintained or enhanced TTR expression (Fig. 2C, lanes 2 to 4; Table 1), as did culturing the endoderm in contact with cardiac mesoderm (Fig. 2C, lane 5). The amounts of FGF-induced liver gene expression were comparable to or greater than that observed when cardiac mesoderm was in contact with the ventral endoderm, relative to the β-actin mRNA internal control.

The hepatogenic effect of FGF1 and FGF2 was specific to the endoderm. Neither factor induced hepatic gene expression in cultured embryo neural tubes, midsections, and head cells (Fig. 2E, lanes 1 to 6; Table 1), all of which originate from the ectoderm, the mesoderm, or both. We conclude that multiple FGFs are expressed in the cardiac mesoderm and are individually sufficient to initiate hepatic gene expression from the endoderm.

To determine whether FGFs are necessary for hepatic specification by the cardiac mesoderm, we sought to perturb FGF signaling by using molecular hybrids between FGF receptors and immunoglobulin G (FR-IgG) (Fig. 3A). These FR-IgG constructs contain the extracellular, ligand binding domain of either FGFR-1 or FGFR-4 fused to the hinge and the dimerization domain of IgG heavy chain, resulting in soluble receptors that sequester FGFs (*28*). FR1-IgG and FR4-IgG molecules were secreted from COS-7 cells, purified from the culture medium (Fig. 3B, lanes 3 and 4), and tested for biological activity (*29*) (Fig. 3C). As would be predicted from the known FGF binding capacity of the intact receptors (*30*), FR1-IgG inhibited the ability of FGF2 to stimulate protein tyrosine kinase activity in NIH 3T3 cells, but FR4-IgG did not (Fig. 3C, lanes 3 to 5). In contrast, FGF8b was efficiently inhibited by FR4-IgG and, to a lesser degree, by FR1-IgG (Fig. 3C, lanes 6 to 8). Thus, the inhibitors exhibit different FGF substrate preferences, as expected from studies with intact FGF receptors (*30*).

Ventral foregut endoderm was dissected from two- to four-somite mouse embryos along with its associated cardiac mesoderm and was cultured in the presence of FR1-IgG or FR4-IgG (500 ng ml^{-1}) alone or in the presence of either protein at 200 ng ml^{-1} with heparan sulfate at 100 ng ml^{-1}. Similar results were obtained under both conditions. As a control, we used either human IgG or

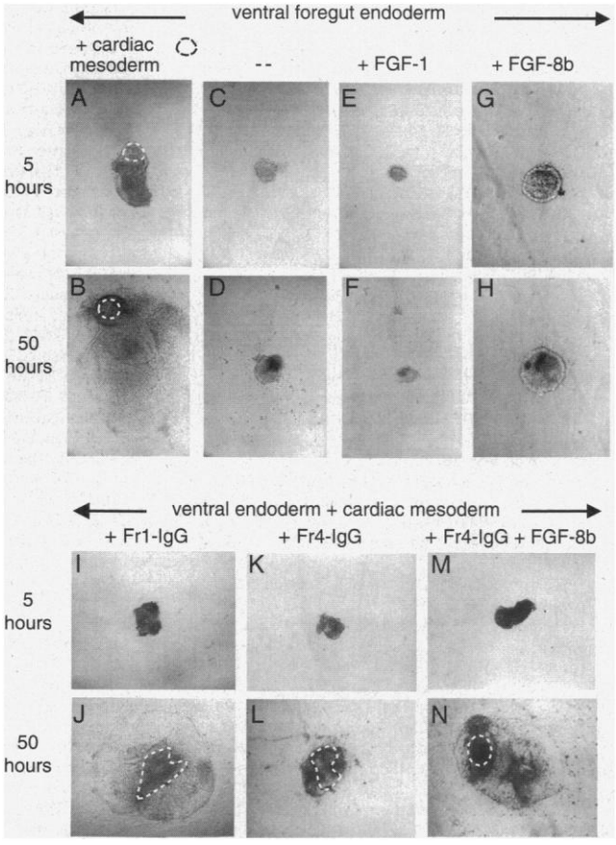

Fig. 4. FGF is necessary for morphological outgrowth of newly specified hepatic endoderm. Micrographs of tissue explants at the designated times after cultures were established. Dashed circles indicate beating cardiac cells. Usually beating areas were not seen at 5 hours. (**A** and **B**) Extensive endodermal outgrowth in cocultures of cardiac mesoderm and foregut endoderm. (**C** to **H**) Ventral foregut endoderm alone shows little outgrowth regardless of the presence of FGFs. (**I** to **N**) Cocultures of ventral foregut endoderm and cardiac mesoderm incubated with the designated components. Original magnification for (A to F, I to N), ×40, and for (G and H) ×100.

buffer containing no fusion proteins. After 2 days in culture, we isolated RNA from individual explants and categorized the amounts of albumin mRNA, relative to actin mRNA as barely detectable (low), comparable to the actin concentration (medium), or greater than the actin concentration (high). In 15 of 20 samples treated with FR1-IgG, albumin concentrations were markedly lower than the control group (Fig. 3, D and E). FR4-IgG was also inhibitory but perhaps slightly less effective (Fig. 3F). The high efficiency of FR1-IgG is consistent with its ability to efficiently inhibit FGF2, which was able to induce liver gene expression on its own. We conclude that endogenous FGF signaling is critical for hepatic induction.

In principle, FGF1 or FGF2 could cause outgrowth of a subpopulation of ventral endoderm cells that were already committed to a hepatic fate and expressing liver-specific genes. Although the high sensitivity of the RT-PCR assay made this unlikely, cardiac mesoderm cultured with foregut endoderm does cause vigorous outgrowth of the endoderm (Fig. 4, A and B), which implicates the presence of morphogenetic signals produced by the cardiac mesoderm (*7*). However, neither FGF1, FGF2, nor FGF8b had a discernible effect on endodermal cell outgrowth (Fig. 4, C to H) (*31*), even though FGF1 and FGF2 potently induced hepatic gene expression (Fig. 2).

Interestingly, in 10 of 14 cultures, FR4-IgG strongly inhibited the morphogenetic response of the endoderm to the cardiac mesoderm (Fig. 4, K and L), whereas FR1-IgG did so in only 3 of 14 samples (Fig. 4, I and J). To test the hypothesis that FR4-IgG was antagonizing an FGF8 isoform, a preferred substrate, we cultured ventral endoderm and cardiac mesoderm fragments in the presence of FR4-IgG and exogenous FGF8b. Remarkably, in five of seven cultures, FGF8b restored the outgrowth response of the foregut endoderm (Fig. 4, M and N). Because FGF8b alone was insufficient to elicit morphogenesis, we conclude that FGF8b, or an FGF with a similar receptor specificity, permits the endoderm to respond to another signal that promotes outgrowth of the newly specified hepatic cells. Preliminary experiments with foregut endoderm alone cultured in FGF2 and FGF8b ($n = 3$) showed that the other signal apparently is not FGF2 (*21*).

We have distinguished two signaling phases in the initiation of liver development from the endoderm. First, FGF signaling from the cardiac mesoderm induces the initial step of hepatogenesis; that is, it initiates the hepatic gene expression program in the ventral foregut endoderm. Based on the cardiac expression of FGF1, FGF2, and FGF8 at the time of hepatic specification and the independent activity of FGF1 and FGF2, hepatic induction appears to result from redundant FGF signaling. Second, early expression of FGF8b or a related molecule appears to potentiate the morphogenetic activity of the nascent hepatic cells. That is, FGF8 works in conjunction with a signal that has not been identified to stimulate cell outgrowth. The two-phase model may apply to other examples of mesodermal patterning of the endoderm during organogenesis, in which initial changes in gene expression are tightly coordinated with, but separable from, the morphogenesis of tissue buds (*1*, *2*).

References and Notes

1. G. K. Gittes and W. J. Rutter, *Proc. Natl. Acad. Sci. U.S.A.* **89**, 1128 (1992); G. Teitelman, S. Alpert, J. M. Polak, A. Martinez, D. Hanahan, *Development* **118**, 1031 (1993); Y. Guz *et al.*, *ibid.* **121**, 11 (1995); U. Ahlgren, J. Jonsson, H. Edlund, *ibid.* **122**, 1409 (1996).
2. R. Gualdi *et al.*, *Genes Dev.* **10**, 1670 (1996).
3. K. Immerglük, P. A. Lawrence, M. Bienz, *Cell* **62**, 261 (1990); R. Reuter, G. E. F. Panganiban, F. M. Hoffman, M. P. Scott, *Development* **110**, 1031 (1990).
4. N. M. Le Douarin, *Med. Biol.* **53**, 427 (1975).
5. S. Fukuda-Taira, *J. Embryol. Exp. Morphol.* **63**, 111 (1981).
6. S.-L. Ang and J. Rossant, *Cell* **78**, 561 (1994); D. C. Weinstein *et al.*, *ibid.*, p. 575; D. Dufort, K. Schwartz, K. Harpal, J. Rossant, *Development* **125**, 3015 (1998); C. T. Kuo *et al.*, *Genes Dev.* **11**, 1048 (1997); J. D. Molkentin, Q. Lin, S. A. Duncan, E. N. Olson, *ibid.*, p. 1061.
7. C. Schmidt *et al.*, *Nature* **373**, 699 (1995); Y. Uehara *et al.*, *ibid.*, p. 702; F. Bladt, D. Riethmacher, S. Isenmann, A. Aguzzi, C. Birchmeier, *ibid.* **376**, 768 (1995); B. Hentsch *et al.*, *Genes Dev.* **10**, 70 (1996); M. Ponţoglio *et al.*, *Cell* **84**, 575 (1996); W. S. Chen *et al.*, *Genes Dev.* **8**, 2466 (1994); F. Hilberg, A. Aguzzi, N. Howells, E. F. Wagner, *Nature* **365**, 179 (1993); A. A. Beg, W. C. Sha, R. T. Bronson, S. Ghosh, D. Baltimore, *ibid.* **376**, 167 (1995); J. Jonsson, L. Carlsson, T. Edlund, H. Edlund, *ibid.* **371**, 606 (1994); M. F. Offield *et al.*, *Development* **122**, 983 (1996); U. Ahlgren, S. L. Pfaff, T. M. Jessell, T. Edlund, H. Edlund, *Nature* **385**, 257 (1997); B. Sosa-Pineda, K. Chowdhury, M. Torres, G. Oliver, P. Gruss, *ibid.* **386**, 399 (1997); S. Kimura *et al.*, *Genes Dev.* **10**, 60 (1996); N. R. Manley and M. R. Capecchi, *Development* **121**, 1989 (1995).
8. S. Cascio and K. S. Zaret, *Development* **113**, 217 (1991); N. Shirojri, J. M. Lemire, N. Fausto, *Cancer Res.* **51**, 2611 (1991).
9. X. Zhu, J. Sasse, D. McAllister, J. Lough, *Dev. Dyn.* **207**, 429 (1996); M. H. Parlow, D. L. Bolender, N. P. Koran-Moore, J. Lough, *Dev. Biol.* **146**, 139 (1991).
10. P. H. Crossley and G. R. Martin, *Development* **121**, 439 (1995).
11. K. L. Stark, J. A. McMahon, A. P. McMahon, *ibid.* **113**, 641 (1991).
12. Y. Sugi, J. Sasse, M. Barron, J. Lough, *Dev. Dyn.* **202**, 115 (1995).
13. T. Maciag, T. Mehlman, R. Friesel, A. B. Schreiber, *Science* **225**, 932 (1984); M. Klagsbrun, *Prog. Growth Factor Res.* **1**, 207 (1989); B. B. Olwin and A. Rapraeger, *J. Cell Biol.* **118**, 631 (1992); A. Bikfalvi *et al. Endocrinol. Rev.* **18**, 26 (1997).
14. E. Amaya, T. J. Musci, M. W. Kirschner, *Cell* **66**, 257 (1991); H. V. Isaacs, M. E. Pownall, J. M. W. Slack, *EMBO J.* **13**, 4469 (1994); T. P. Yamaguchi, K. Harpal, M. Henkemeyer, J. Rossant, *Genes Dev.* **8**, 3032 (1994).
15. J. Erickson, S. Norlin, T. M. Jessell, T. Edlund, *Development* **125**, 1005 (1998).
16. P. H. Crossley, G. Minowada, C. A. MacArthur, G. R. Martin, *Cell* **84**, 127 (1996); H. Ohuchi *et al.*, *Development* **124**, 2235 (1997); K. Peters *et al.*, *EMBO J.* **13**, 3296; H. Nogawa and T. Ito, *Development* **121**, 1015 (1995); S. Bellusci *et al.*, *ibid* **124**, 4867 (1997); W. V. Cardoso *et al.*, *Dev. Dyn.* **208**, 398 (1997); H. Ohuchi *et al.*, *Development* **124**, 2235 (1997); H. Min *et al.*, *Genes Dev.* **12**, 3156 (1998); A. Neubuser, H. Peters, R. Balling, G. R. Martin, *Cell* **90**, 247 (1997); P. Kettunen and I. Thesleff, *Dev. Dyn.* **211**, 256 (1998).
17. T. P. Yamaguchi *et al.*, *Genes Dev.* **8**, 3032 (1994); C. X. Deng *et al.*, *ibid.*, p. 3045; E. N. Meyers, M. Lewandoski, G. R. Martin, *Nature Genet.* **18**, 136 (1998).
18. S. Ortega *et al.*, *Proc. Natl. Acad. Sci. U.S.A.* **95**, 5672 (1998); R. Dono *et al.*, *EMBO J.* **17**, 4213 (1998); M. Weinstein, X. Xu, K. Ohyama, C. X. Deng, *Development* **125**, 3615 (1998).
19. Whole-mount in situ hybridization was performed as described [H. Sasaki and B. L. M. Hogan, *Development* **118**, 47 (1993)]. Full-length *Fgf1*, *Fgf2* cDNAs (provided by Gail Martin) and a 400-nucleotide *Fgf8* cDNA (*10*) were used to generate digoxigenin-labeled antisense probes.
20. Antibody staining was performed as reported [T. Ohta *et al.*, *Br. J. Cancer* **72**, 824 (1995)] with modifications. Embryos were fixed in 70% EtOH overnight at 4°C, embedded in a paraffin block, and sectioned 5 μm thick. For FGF1 and FGF2 localization, sections were treated with 0.25% trypsin in phosphate-buffered saline (PBS) for 5 min at room temperature. Mouse monoclonal antibodies against FGF1 were obtained from Sigma, and monoclonal antibody against FGF2, bFM-2, has been described [K. Matsuzaki *et al.*, **86**, 9911 (1989); provided by K. Matsumoto]. For FGF8 localization, sections were microwaved in 10 mM sodium citrate buffer to unmask antigens. Mouse monoclonal antibody against FGF8 was obtained from R&D systems. Normal mouse IgG was used as a control. For the staining of FGFR-1 and -4, we used rabbit polyclonal antibodies from Santa Cruz and normal rabbit IgG. In all cases, we used alkaline phosphatase–conjugated secondary antibodies (Sigma). We counterstained some sections with eosin Y.
21. J. Jung, M. Zheng, K. Zaret, unpublished observations.
22. The dissection, culture, and analysis of C3H mouse embryo tissues was as described (*2*). About one-half the embryos at 8 to 8.5 days of gestation contained two to six somites, one-half of those yielded successful endoderm isolations, and two-thirds of those yielded sufficient cells in explants for RNA isolation. Enzymatic digestion [E. Houssaint, *Cell Differ.* **9**, 269 (1980)] was used in most cases to enhance the purity of ventral endoderm tissue; the enzyme treatment had no effect on hepatic induction. Anterior portions of the embryos were isolated and incubated in a solution of 0.025% trypsin, 0.125% pancreatin, 0.025% polyvinylpyrrolidone-40, 20 mM Hepes (pH 7.4) in PBS at 4°C for 3 to 5 min. The tissues were transferred to Dulbecco's modified Eagle's medium (DMEM) containing 10% calf serum at 37°C for 1 min to stop the digestion. The tissue was then transferred to PBS on a dissecting dish and the ventral foregut endoderm was separated from cardiac mesoderm with tungsten needles under a dissecting microscope at ×60 magnification. Tissues were cultured on collagen-coated slide microwells (*2*) in DMEM containing 10% calf serum (Hyclone). Cells were cultivated for 2 days at 37°C before analysis.
23. FGF test medium included heparan sulfate (50 ng ml^{-1}) [L. Niswander and G. R. Martin, *Nature* **361**, 68 (1993)] and 0.1% bovine serum albumin with the designated concentrations of recombinant human FGF1 or FGF2 (Boehringer Mannheim) or recombinant mouse FGF8b (R&D systems).
24. RNA was isolated from individual colonies and subjected to RT-PCR analysis as described (*7*), except that the sequence of the β-actin mRNA sense-strand oligonucleotide was 5′-AAAGACCTGTACGCCAACACAGTG-3′. The oligonucleotide sequences for analysis of TTR mRNA were 5′-CTTCCCTTCGACTCTTCCTCCT-3′ (sense strand) and 5′-GCCACGTCTACAGCAGGGCTGC-3′ (antisense strand). Actin primers were added after seven cycle steps with the liver-specific primers. Reaction products were tested from different cycle steps and only those samples within the exponential range of the PCR were used for the analysis.
25. J. K. Wang, G. Gao, M. Goldfarb, *Mol. Cell. Biol.* **14**, 181 (1994).
26. J. B. A. Green, H. V. New, J. C. Smith, *Cell* **71**, 731 (1992).
27. A. Makover, D. R. Soprano, M. L. Wyatt, D. S. Goodman, *Differentiation* **40**, 17 (1989).
28. A. S. Tucker *et al.*, *Eur. J. Oral Sci.* **106** (Suppl. 1), 122 (1998); G. Celli *et al.*, *EMBO J.* **17**, 1642 (1998).
29. Plasmid DNAs encoding FR-IgG fusion proteins were transiently transfected into COS-7 cells and secreted

proteins were purified with protein A–Sepharose beads. Proteins were quantitated by dot immunoblot analysis by using conjugated antibody to human IgG–horseradish peroxidase (Jackson ImmunoResearch Lab). Protein purity was analyzed by SDS–polyacrylamide gel electrophoresis (PAGE) and silver staining. Ligand binding specificity of the proteins was assessed with NIH 3T3 cells. Briefly, serum-starved cells were stimulated with FGFs in the presence of either FR1-IgG or FR4-IgG for 5 hours. Total cell lysates were prepared and the changes in the protein phosphorylation profile were determined by immunoblot analysis with an antibody to phosphotyrosine (Santa Cruz).

30. D. M. Ornitz *et al.*, *J. Biol. Chem.* **271**, 15292 (1996); C. A. Dionne *et al.*, *EMBO J.* **9**, 2685 (1990).
31. Data not shown for FGF2.
32. S. Sell, M. A. Longley, J. Boulter, *Dev. Br. Res.* **22**, 49 (1985); A. Poliard, G. Feldman, D. Bernau, *Differentiation* **39**, 59 (1988); J. Nahon *et al.*, *J. Biol. Chem.* **263**, 11436 (1988).
33. Supported by National Institutes of Health grant GM36477 to K.S.Z. We thank G. Martin for the FGF cDNAs; K. Matsumoto for FGF2 monoclonal antibody; and J. Coleman, P. Bossard, and J. Lora for comments on the manuscript.

22 February 1999; accepted 13 May 1999

Identification of Both Shared and Distinct Proteins in the Major and Minor Spliceosomes

Cindy L. Will,[1] Claudia Schneider,[1] Robin Reed,[2] Reinhard Lührmann[1,3]*

In metazoans, two distinct spliceosomes catalyzing pre–messenger RNA splicing have been identified. Here, the human U11/U12 small nuclear ribonucleoprotein (snRNP), a subunit of the minor (U12-dependent) spliceosome, was isolated. Twenty U11/U12 proteins were identified, including subsets unique to the minor spliceosome or common to both spliceosomes. Common proteins include four U2 snRNP polypeptides that constitute the essential splicing factor SF3b. A 35-kilodalton U11-associated protein homologous to the U1 snRNP 70K protein was also identified. These data provide fundamental information about proteins of the minor spliceosome and shed light on its evolutionary relationship to the major spliceosome.

The minor (U12-dependent) spliceosome is required for splicing a rare class of nuclear pre-mRNA introns (*1*). These so-called U12-type introns contain highly conserved sequence elements at the 5′ splice site and branch site that are distinct from the weakly conserved sequence elements found in the major class of pre-mRNA introns (*1*, *2*). During assembly of the minor spliceosome, the U11 snRNP forms base pairs with the 5′ splice site, and the U12 snRNP forms base pairs with the branch site, analogous to the U1 and U2 snRNPs in the major spliceosome (*3*). Subsequently, mature spliceosomes are formed by the association of the U5 and U4atac/U6atac snRNPs (*4*). In the major spliceosome, 5′ splice site and branch site recognition are mediated by multiple interactions involving both RNA and protein (*5*). In metazoans, formation of the U1 snRNA/5′ splice site duplex is facilitated by several polypeptides, including the U1 snRNP 70K and C proteins, as well as members of the SR (serine- and arginine-rich) protein family (*6*). Similarly, base pairing between U2 snRNA and the branch site requires numerous U2 snRNP proteins, in particular the subunits of the heteromeric splicing factors SF3a and SF3b (*5*–*7*).

In contrast to their counterparts in the major spliceosome, the U11 and U12 snRNPs are present in nuclear extract not only as individual monoparticles, but also as a highly stable 18*S* U11/U12 complex (*8*). Recent in vitro binding studies suggest that U11 and U12 interact with the pre-mRNA as a preformed complex (*9*). This observation, coupled with the fact that U12-type introns lack the essential pyrimidine tract found at the 3′ splice site of the major class of introns, suggests that differences may exist in the mechanism of initial splice site recognition and pairing in the two types of spliceosomes. To identify proteins involved in this process in the minor spliceosome, we have characterized polypeptides associated with the human 18*S* U11/U12 snRNP complex.

Spliceosomal snRNPs were immunoaffinity-purified from HeLa nuclear extract and fractionated by glycerol gradient sedimentation. From the 18*S* region of the gradient, U11/U12 snRNP complexes were then affinity-selected using biotinylated 2′-*O*-methyl oligonucleotides and streptavidin agarose (*10*). snRNPs containing predominantly U11 and U12 snRNA were selected by oligonucleotides complementary to nucleotides 2 to 18 of the U11 snRNA (Fig. 1A, lane 2) or nucleotides 11 to 28 of the U12 snRNA (Fig. 1A, lane 3). The coselection of U12 with an oligonucleotide directed against U11, and vice versa, indicated that mainly 18*S* U11/U12 snRNP complexes (as opposed to U11 or U12 monoparticles) had been selected. Consistent with this conclusion, the U11/U12 snRNPs selected by either oligonucleotide exhibited identical protein patterns (Fig. 1B, lanes 2 and 3). Twenty distinct proteins were detected in the U11/U12 complex. Eight of these comigrated with the snRNP Sm proteins B′, B, D3, D2, D1, E, F, and G, which are present in the major spliceosomal snRNPs (Fig. 1B, lanes 1 to 3; see also Fig. 2) (*11*). Antibodies reacting specifically with B′/B, D3, D2, F, or G also recognized proteins of identical molecular mass on immunoblots of the U11/U12 complex (*12*). These data indicate that U11/U12 contains the same eight Sm proteins

Table 1. U2 snRNP proteins are also present in U11/U12 snRNPs. X indicates an unidentified amino acid (*28*). Mismatches (indicated by boldface letters) were observed between the U11/U12-160kD and U2-160kD proteins at position 149 (V versus A) and between the U11/U12-130kD and U2-120kD proteins at positions 1209, 1211, and 1212 (D versus N, R versus A, and T versus Q, respectively).

U11/U12 protein	Peptides	Identity	Reference	Amino acids
160 kD	KMN**A**RTYMDVMREQHLTK	U2-160kD	(*16*)	146–162
	KLTATPTPLGGMTGF			428–442
	KAIVNVIGMH			997–1007
150 kD	KRIFEAFK	U2-150kD	(*17*)	364–371
	KLRRMNRFTVAE			430–441
	KRTGIQEMREALQEK			506–520
	KLTIHGDLYYEG			560–571
130 kD	KLGAVFNQVAFPLQYT	U2-120kD	(*29*)	768–783
	KLLRVYDLGK			964–973
	KNVSEELDRTPPEVSK			1190–1205
	KLE**NIAQ**RYAF			1206–1217
49 kD	KVSEPLLXELFLQ	U2-53kD	(*18*)	23–35
	KDRVTGQHQGYGFVEFLSEE			46–65

[1]Institut für Molekularbiologie und Tumorforschung, Philipps-Universität, 35037 Marburg, Germany. [2]Department of Cell Biology, Harvard Medical School, Boston, MA 02115, USA. [3]Department of Cellular Biochemistry, Max Planck Institute of Biophysical Chemistry, 37070 Göttingen, Germany.

*To whom correspondence should be addressed. E-mail: luehrmann@imt.uni-marburg.de